



Impacts of climate change from 2000 to 2050 on wildfire activity and carbonaceous aerosol concentrations in the western United States

D. V. Spracklen,^{1,2} L. J. Mickley,¹ J. A. Logan,¹ R. C. Hudman,^{1,3} R. Yevich,¹ M. D. Flannigan,⁴ and A. L. Westerling⁵

Received 9 August 2008; revised 26 March 2009; accepted 18 June 2009; published 20 October 2009.

[1] We investigate the impact of climate change on wildfire activity and carbonaceous aerosol concentrations in the western United States. We regress observed area burned onto observed meteorological fields and fire indices from the Canadian Fire Weather Index system and find that May–October mean temperature and fuel moisture explain 24–57% of the variance in annual area burned in this region. Applying meteorological fields calculated by a general circulation model (GCM) to our regression model, we show that increases in temperature cause annual mean area burned in the western United States to increase by 54% by the 2050s relative to the present day. Changes in area burned are ecosystem dependent, with the forests of the Pacific Northwest and Rocky Mountains experiencing the greatest increases of 78 and 175%, respectively. Increased area burned results in near doubling of wildfire carbonaceous aerosol emissions by midcentury. Using a chemical transport model driven by meteorology from the same GCM, we calculate that climate change will increase summertime organic carbon (OC) aerosol concentrations over the western United States by 40% and elemental carbon (EC) concentrations by 20% from 2000 to 2050. Most of this increase (75% for OC and 95% for EC) is caused by larger wildfire emissions with the rest caused by changes in meteorology and for OC by increased monoterpene emissions in a warmer climate. Such an increase in carbonaceous aerosol would have important consequences for western U.S. air quality and visibility.

Citation: Spracklen, D. V., L. J. Mickley, J. A. Logan, R. C. Hudman, R. Yevich, M. D. Flannigan, and A. L. Westerling (2009), Impacts of climate change from 2000 to 2050 on wildfire activity and carbonaceous aerosol concentrations in the western United States, *J. Geophys. Res.*, 114, D20301, doi:10.1029/2008JD010966.

1. Introduction

[2] Emissions from wildfires in North America can have important consequences for air quality both regionally [McMeeking *et al.*, 2005, 2006; McKenzie *et al.*, 2006; Hodzic *et al.*, 2007; Park *et al.*, 2007; Spracklen *et al.*, 2007; Jaffe *et al.*, 2008b, 2008a; Pfister *et al.*, 2008] and at sites thousands of kilometers from the fire [Wotowa and Trainer, 2000; DeBell *et al.*, 2004; Jaffe *et al.*, 2004; Lapina *et al.*, 2006; Val Martin *et al.*, 2006; Duck *et al.*, 2007; Lewis *et al.*, 2007]. Wildfire activity in North America is largely controlled by temperature and precipitation [e.g.,

Balling *et al.*, 1992; Gedalof *et al.*, 2005] which are in turn partly driven by large-scale ocean circulation patterns [e.g., Skinner *et al.*, 1999; Duffy *et al.*, 2005; Skinner *et al.*, 2006]. Climate change therefore has the potential to influence the frequency, severity, and extent of wildfires [e.g., Flannigan *et al.*, 2005]. In this study we use stepwise linear regression to evaluate relationships between the area burned by wildfires and variables chosen from observed meteorology and standard fire indices. We apply these relationships to meteorological fields calculated by a general circulation model (GCM) for 2000–2050 to determine the effect of changing climate on future area burned. Finally, we use a global chemistry model, driven by the GCM, to assess the impact of wildfires in a future climate on carbonaceous aerosols in the western United States.

[3] Records of wildfire show increasing area burned in Canada [Stocks *et al.*, 2002; Gillett *et al.*, 2004; Kasischke and Turetsky, 2006], Alaska [Kasischke and Turetsky, 2006], and the western United States [Westerling *et al.*, 2006] over the past few decades. In the western United States the annual area burned by large forest wildfires (>400 ha) during 1987 to 2003 was more than 6 times that during 1970 to 1986 [Westerling *et al.*, 2006]. Wildfire behavior is modified by climate, forest management, and

¹School of Engineering and Applied Sciences, Harvard University, Cambridge, Massachusetts, USA.

²Now at Institute for Atmospheric Science, School of Earth and Environment, University of Leeds, Leeds, UK.

³Now at Department of Chemistry, University of California, Berkeley, California, USA.

⁴Great Lakes Forestry Centre, Canadian Forest Service, Sault Ste. Marie, Ontario, Canada.

⁵Sierra Nevada Research Institute, University of California, Merced, California, USA.

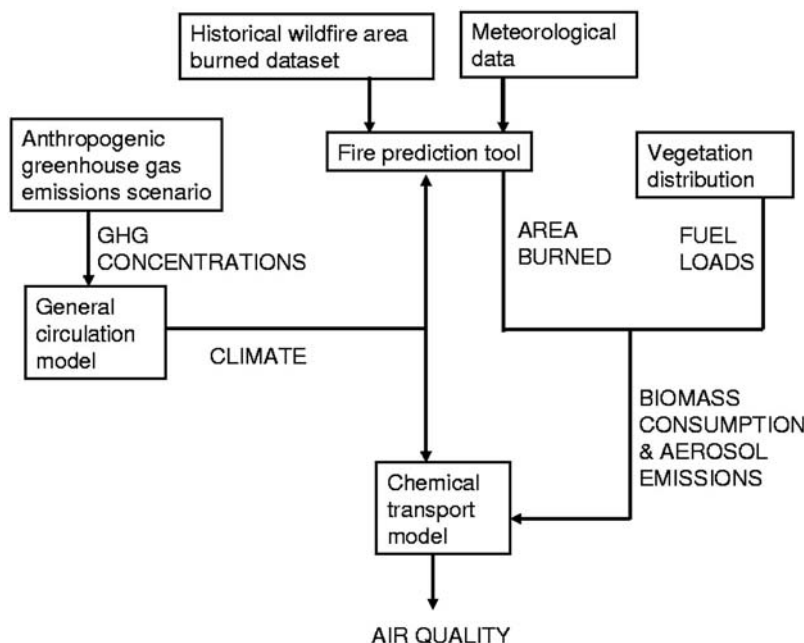


Figure 1. Schematic of our approach to modeling the impact climate change on future wildfires and carbonaceous aerosol concentrations.

fire suppression [Allen *et al.*, 2002; Noss *et al.*, 2006], and understanding the reasons for changing wildfire is further complicated by changes in fire reporting over the period of record. However, recent changes in climate were likely the main drivers for increases in area burned both in the western United States [Westerling *et al.*, 2006] and Canada [Gillett *et al.*, 2004; Kasischke and Turetsky, 2006; Girardin, 2007]. For the western United States, Westerling *et al.* [2006] showed that the observed increase in wildfire has been driven largely by earlier spring snowmelt and increasing spring and summertime temperatures; mean March–August temperatures for 1987–2003 were 0.87 K warmer than those in 1970–1986.

[4] Several studies have estimated the impacts of future climate change on wildfire. Flannigan and Van Wagner [1991] used three different GCMs to predict on average a 46% increase in seasonal severity rating (SSR, a measure of fire weather) across Canada under a $2 \times \text{CO}_2$ scenario. Similar results were found by Flannigan *et al.* [2000] who used two GCMs to predict a 10–50% increase in SSR across much of North America under the same scenario. Longer future fire seasons in Canada were predicted by Stocks *et al.* [1998] and Wotton and Flannigan [1993]. Increased future fire danger has also been predicted for Russia [Stocks *et al.*, 1998], the western United States [Brown *et al.*, 2004; Westerling and Bryant, 2008], and the European Mediterranean area [Moriondo *et al.*, 2006]. Westerling and Bryant [2008] predict a 10–35% increase in large fire risk by midcentury in California and Nevada, depending on the greenhouse gas emissions scenario and GCM used. Large regional variation in future wildfires is predicted by Regional Climate Models (RCMs), including decreased fire danger in parts of eastern Canada due to increased precipitation [Bergeron and Flannigan, 1995; Flannigan *et al.*, 2001].

[5] Many of the above studies predict changes in fire indices, but estimates of emissions from fires require predictions of area burned. Flannigan *et al.* [2005] investigated relationships between climate and the areas of fires in Canada. Stepwise linear regression was used to derive the best predictors of area burned, chosen from meteorological variables (surface temperature, rainfall, wind speed, and relative humidity) and calculated values of forest fuel moisture from the Canadian Fire Weather Index (FWI) System. Temperature and fuel moisture explained between 36 and 64% of the variance in monthly area burned depending on the ecosystem. The Canadian and Hadley Centre GCMs were used to predict increases in area burned of 74–118% under a $3 \times \text{CO}_2$ scenario. RCMs have also been used to study wildfire area burned in limited regions of Canada. For the boreal forests of Alberta, Tymstra *et al.* [2007] used an RCM to predict a 13% increase in area burned in a $2 \times \text{CO}_2$ scenario and a 30% increase in a $3 \times \text{CO}_2$ scenario. Most of these studies did not account for any future changes in ignition sources. Price and Rind [1994] used empirical lightning and fire models along with the Goddard Institute for Space Studies (GISS) GCM to predict that more intense convection under a $2 \times \text{CO}_2$ scenario leads to increased lightning and a 78% increase in area burned in the United States.

[6] Despite these efforts to predict the effect of future climate on wildfires, there have not been studies of the impact of these future wildfires on air quality. In this paper we predict how wildfires in the western United States will respond to changes in climate between the present day and 2050 and evaluate the impacts on aerosol air quality (see Figure 1). We apply the technique of Flannigan *et al.* [2005] to the western United States, building regressions between observed wildfire area burned [Westerling *et al.*, 2003] and observed climate. Projections of future climate, calculated by the GISS GCM, are used to predict changes in

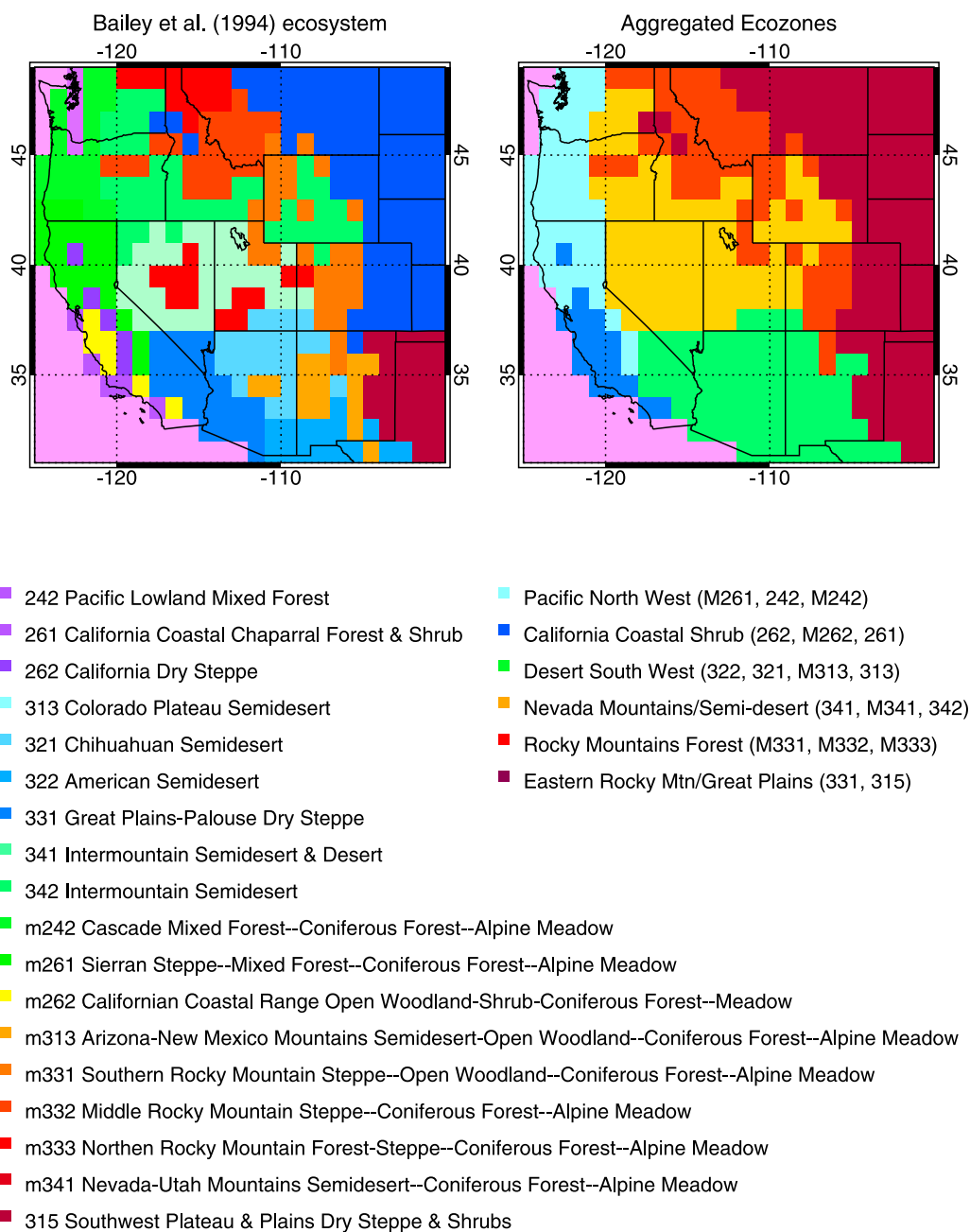


Figure 2. Ecosystems in the western United States. (left) *Bailey et al.* [1994] ecosystem classes projected onto a 1° by 1° grid. (right) Aggregated ecosystems that are used in this analysis: Pacific Northwest, Californian Coastal Shrub, Desert Southwest, Nevada Mountains/Semidesert, Rocky Mountains Forest, and Eastern Rocky Mountains/Great Plains.

wildfire area burned. We use the GEOS-Chem chemical transport model (CTM) driven by meteorology from the GISS model to quantify the impact of changing wildfire on carbonaceous aerosol concentrations.

2. Predicting Wildfire Emissions for 2000–2050

[7] Here we describe our prediction of future wildfire emissions of carbonaceous aerosol in the western United States, defined as the domain 31° – 49° N, 125° – 100° W (from the Pacific Coast to eastern Colorado and from the Mexican border to the Canadian border).

2.1. Area Burned Predictions

[8] We extend the approach of *Flannigan et al.* [2005] to the western United States, building regressions of observed area burned with surface meteorological data and output from the FWI model. Observed area burned was taken from the database of *Westerling et al.* [2003]. They used reports from various agencies in the United States that provided the area burned on federal land, and the start and end date of individual fires, from 1980 to 2000. This database has been extended to 2004. *Westerling et al.* [2003] assumed that the fires burn entirely in the month during which they started

Table 1. Wildfire Area Burned Regressions for Aggregated Ecoregions in the Western United States^a

| Ecoregion | Bailey Ecosystem Classes ^b | Mean Elevation (m) | Number of Met Stations | R ² | Predicted Area Burned/ha ^c |
|--------------------------------------|---------------------------------------|--------------------|------------------------|----------------|---|
| Pacific Northwest | M261,242,M242 | 1040 | 94 | 52% | $= -3.1 \times 10^6 + 9.4 \times 10^4 T + 1.7 \times 10^3 DC$ |
| California Coastal Shrub | 262,M262,261 | 635 | 32 | 24% | $= -3.6 \times 10^6 + 3.4 \times 10^4 T_{\max} + 2.6 \times 10^4 FFMC$ |
| Desert Southwest | 322,321,M313,313 | 1600 | 61 | 49% | $= -1.64 \times 10^6 + 6.3 \times 10^4 T + 296 DC_{\max}$ |
| Nevada Mountains/Semidesert | 341,M341,342 | 1740 | 22 | 37% | $= 3.9 \times 10^5 + 1.2 \times 10^4 FWI_{\max} - 1.4 \times 10^6 Rain$ |
| Rocky Mountains Forest | M331,M332,M333 | 1760 | 60 | 48% | $= -6.55 \times 10^6 + 3.2 \times 10^5 T + 5.3 \times 10^3 BUI_{\max}$ |
| Eastern Rocky Mountains/Great Plains | 331, 315 | 1300 | 8 | 57% | $= -3.6 \times 10^5 + 3.4 \times 10^4 DSR$ |

^aFrom Bailey *et al.* [1994] ecosystem classes.

^bDescription of Bailey ecosystems appears in Figure 1. For each ecoregion the number of meteorological stations and the mean elevation of the stations above sea level is shown.

^cPredictors are chosen from maximum and mean daily May through October values of meteorological variables and components of the Canadian Fire Weather Index System (see Figure 3): T (°C), Temperature; DC, Drought Code; FFMC, Fine Fuel Moisture Code; FWI, Fire Weather Index; Rain, accumulated 24-h rainfall (mm); BUI, Build-up Index; DSR, Daily Severity Rating.

(end dates are often unreliable), and the areas were aggregated on a grid of $1^\circ \times 1^\circ$. Because the gridded database used only the start date of each fire, it may not accurately reflect the seasonal dependence of each fire season. In addition, the wildfire time series is relatively short, and if there are only a few extreme events, it is difficult to fit with the least squares approach used here. For these reasons we chose to predict annual area burned.

[9] Area burned was binned according to the ecological stratification of Bailey *et al.* [1994]. This system defines 18 ecoprovinces in the western United States. These ecosystems were further aggregated to produce six ecoregions with similar vegetation and climate, as shown in Figure 2. We tested our regressions with the original 18 ecosystems, but found we could better fit area burned for the larger ecoregions, as did Flannigan *et al.* [2005] for Canada. This is probably caused by meteorological factors that influence area burned operating at synoptic scales, and larger spatial units providing some statistical smoothing of noisy data for area burned. Littell *et al.* [2009] find strong relationships (R^2 of between 0.31 and 0.87) at the original ecoprovince level, potentially because they also include the Palmer Drought Severity Index and antecedent meteorological variables within their regressions, and because they first extracted the principal components of the times series of meteorological data before fitting the area burned data. The coarse spatial resolution of the global climate model limits the scale at which we can make future projections of climate and so area burned. For this reason we use the six aggregated ecoregions (Pacific Northwest, California Coastal Shrub, Desert Southwest, Nevada Mountains/Semidesert, Rocky Mountains Forest, and Eastern Rocky Mountains/Great Plains) for the rest of this work.

[10] We obtained from the USDA Forest Service data for four meteorological variables important to wildfire frequency and required as input to the FWI model: daily 12.00 local standard time temperature, relative humidity, wind speed, and 24-h accumulated rainfall (available at <http://fam.nwcg.gov/fam-web/weatherfirecd/>). Meteorological stations were selected if they reported data for at least two thirds of the 1980–2004 time period and if the altitude of the station was within 500 m of the mean altitude of all stations within that ecoregion. Table 1 shows the number of stations selected for each ecoregion. Temperature and relative humidity values at each station were adjusted to the mean elevation of the stations. For temperature the adjustment is based on the U.S. Standard Atmosphere lapse rate of -6.5 K/km. Relative humidity was then recalculated using the adjusted temperature. For 1980–2004 we calculated a daily value for each meteorological variable and each ecoregion as an average across the selected meteorological stations for each ecoregion.

[11] The calculated daily values of the four meteorological variables were used as input to the Canadian FWI System [Van Wagner, 1987]. The model calculates daily fuel moisture codes and fire severity indices using these four variables to track changes in forest fuel moisture. A schematic of this model is shown in Figure 3. The fuel moisture codes describe the moisture content of three distinct fuel layers in the forest floor. The Fine Fuel Moisture Code (FFMC) represents surface fuel litter and changes rapidly with short-term changes in atmospheric moisture (time lag

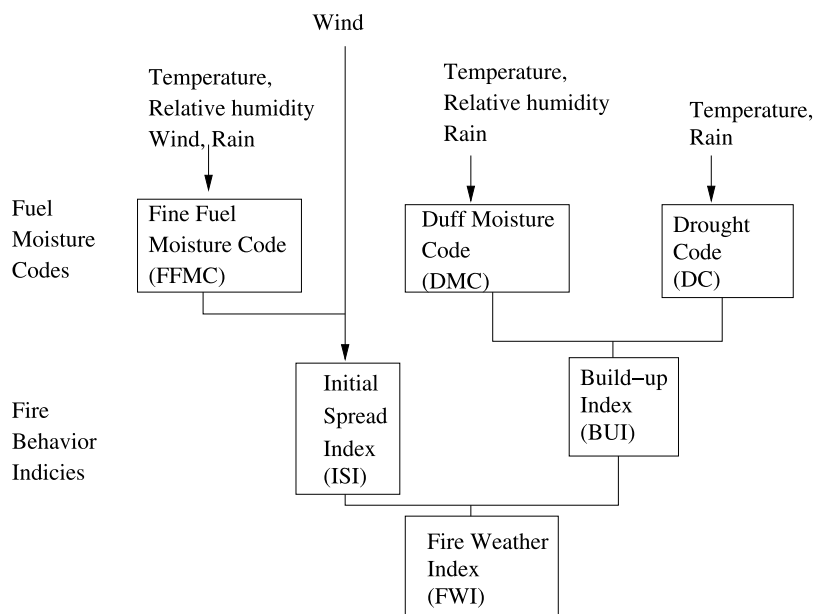


Figure 3. Schematic of the Canadian Fire Weather Index (FWI) System.

of 2/3 day). The Duff Moisture Code (DMC) represents loosely compacted organic layers (time lag of 15 days) and the Drought Code (DC) represents deep layers of compacted fuel and reacts to seasonal droughts (time lag of 52 days). The fire severity ratings combine information from the fuel moisture codes to give an indication of the fire danger or rate of fire spread. The Build-up Index (BUI) combines DMC and DC and is an indication of the availability of fuel for consumption. The potential rate of spread of a fire is calculated by combining wind speed and FFMC to give the Initial Spread Index (ISI). The ISI and BUI are combined to give the Fire Weather Index (FWI) which is commonly used as a general index of fire danger. The Daily Severity Rating (DSR) is an exponential function of the FWI and gives an indication of the difficulty of fire control.

[12] Linear forward stepwise regression was used for each of the six ecoregions with annual area burned as the predictand. For predictors we used the maximum and mean of the daily May to October values of temperature, relative humidity, and wind speed and the seven output fields from the FWI model (described in section 2.1). In addition we used May to October mean daily rainfall and total May to October rainfall. This gives 22 potential predictors. We used the same test for significance as *Flannigan et al.* [2005]; terms were accepted only if they met a significance level (p value) of 0.15. The predictor with the highest correlation coefficient was added to the regression first. Predictors were then added in the order that maximized the correlation coefficient, until the correlation coefficient did not increase by a preselected amount (typically 2%), or until a predictor was selected that resulted in a nonphysical (counterintuitive) relationship between area burned and fuel moisture. In general, two predictors were selected for each ecoregion. We tested our method using both area burned and natural logarithm of area burned. We found similar correlation coefficients with the two predictands. For the rest of this work, prediction of linear area burned was used.

[13] Figure 4 shows a comparison of observed and predicted annual area burned in the Pacific Northwest and Rocky Mountains Forest ecoregions. The observations show large interannual variability in area burned, with a range of 7500 ha/a to 440,000 ha/a in the Pacific Northwest and 4800 ha/a to 1.45 million ha/a in the Rocky Mountains Forest. In the Pacific Northwest the regression explains 52% of this interannual variability. The chosen predictors for this region are mean drought code and mean temperature, which correlate with area burned with R^2 of 46 and 43%, respectively. The greatest observed area burned occurred in 1987 and 2002 coincident with high DC and T. Predicted area burned is also maximum during these 2 years but is underestimated by about 40%. In the Rocky Mountains Forest the regression explains 47% of the variability in annual area burned. The best predictors for this region are mean temperature and maximum Build-up Index, which correlate with area burned with R^2 of 42 and 40%, respectively. The regression underpredicts the largest fire year in 1988 by about 60%, but other large fire years (e.g., 2000 and 2001) are well predicted.

[14] Table 1 shows the best predictors and the explained variance for the six ecoregions in the western United States. The regressions explain 24–57% (mean 45%) of variance in annual area burned. Our relationships are weaker than recent work by *Littell et al.* [2009] who found 33–87% (mean 64%) for the reasons discussed earlier in this section. The explained variance in our work is generally greater in forest dominated ecosystems (48–52%) than in shrub and grass dominated ecosystems (24–49%). The lower explained variance in these ecosystems is likely due to the importance of the previous year's climate for fire activity in these areas [*Westerling et al.*, 2002; *Westerling and Bryant*, 2008; *Littell et al.*, 2009] which we do not take into account with our method. However, as we show in section 2.3, these shrub and grass dominated ecosystems have limited impact on regional particulate air quality because of low fuel loads.

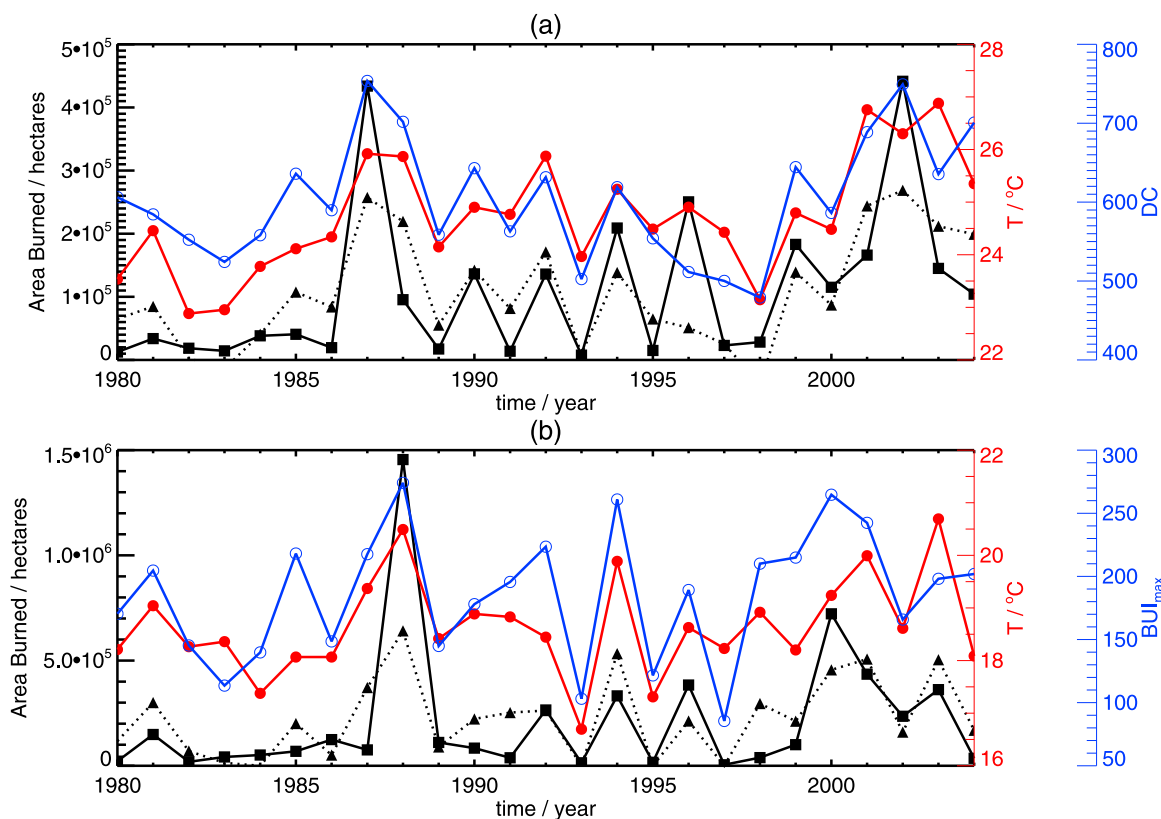


Figure 4. Observed (*Westerling et al.* [2003], filled squares) and predicted (stepwise linear regression, filled triangles) annual area burned between 1980 and 2004 in (a) Pacific Northwest and (b) Rocky Mountains Forest ecoregions (see Figure 2 for locations). Also shown are the predictors chosen by the regression (mean or maximum of the daily values for May to October): mean temperature (T , filled circles), and indices from the Canadian FWI System (see Figure 3, open circles): mean Drought Code (DC) and maximum Build-up Index (BUI_{max}).

[15] Best predictors of area burned are ecosystem dependent but generally include temperature and fuel moisture codes (FFMC or DC). Temperature is the most commonly chosen predictor in the western United States, as has been found previously in Canada [*Flannigan et al.*, 2005]. High temperatures are associated with clear skies, persistent stagnation, and dry fuel: conditions that favor wildfire occurrence.

2.2. Simulation of Future Area Burned

[16] To calculate future area burned, we archived daily mean temperature, relative humidity, and local noon wind speed as well as 24-h accumulated rainfall from the GISS simulation for 2000–2050. We used the “ q flux” version of the GISS GCM 3 [*Rind et al.*, 2007], which has a horizontal resolution of $4^\circ \times 5^\circ$ and 23 vertical sigma levels between the surface and 0.002 hPa. In the q flux version, ocean heat transport fluxes are kept fixed while ocean temperatures and ocean ice respond to changes in climate. Observed concentrations of well-mixed greenhouse gases, ozone, and aerosols were used for the model spin-up between 1950 and 2000, starting from a climate equilibrium [*Hansen et al.*, 2002]. For 2001 to 2055 we used concentrations of well-mixed greenhouse gases from the IPCC SRES A1B scenario, with CO_2 calculated using the Bern-CC model [*Houghton*, 2001]. Under this scenario, CO_2 mixing ratios reach

522 ppm by 2050. We assumed no changes in ozone or aerosols from 2001 to 2055 for the purpose of calculating climate change. This model predicts global mean July temperatures to increase by $1.8^\circ C$ from 2000 to 2050.

[17] Because the GISS GCMs tend to have a warm continental bias [*Schmidt et al.*, 2006], we scaled temperature as well as the other fields to match observations by multiplying the GISS output by the ratio of mean observed to mean GISS values in each model grid square for May to October of 1990–2000. The adjusted GISS meteorology was used as input for the FWI model to calculate daily fuel moisture parameters. The regressions developed in section 2.1 were then applied to GISS and FWI output to predict ecosystem specific annual area burned.

[18] Figure 5 shows the simulated changes between 2000 and 2050 in mean May through October noon values of the four meteorological variables over the western United States; we compare the means for 1996–2005 and for 2046–2055. Temperatures increase across the western United States by 1 – $3^\circ C$, with the largest increases in the Pacific Northwest and Nevada Mountains/Semidesert ecoregions. The projected change in temperature over the western United States is large, 1.5–1.8 times the standard deviation in May–October mean temperature, even though 2049 has a mean temperature below the 1996–2006 mean. Precipitation and relative humidity increase by 7% and less

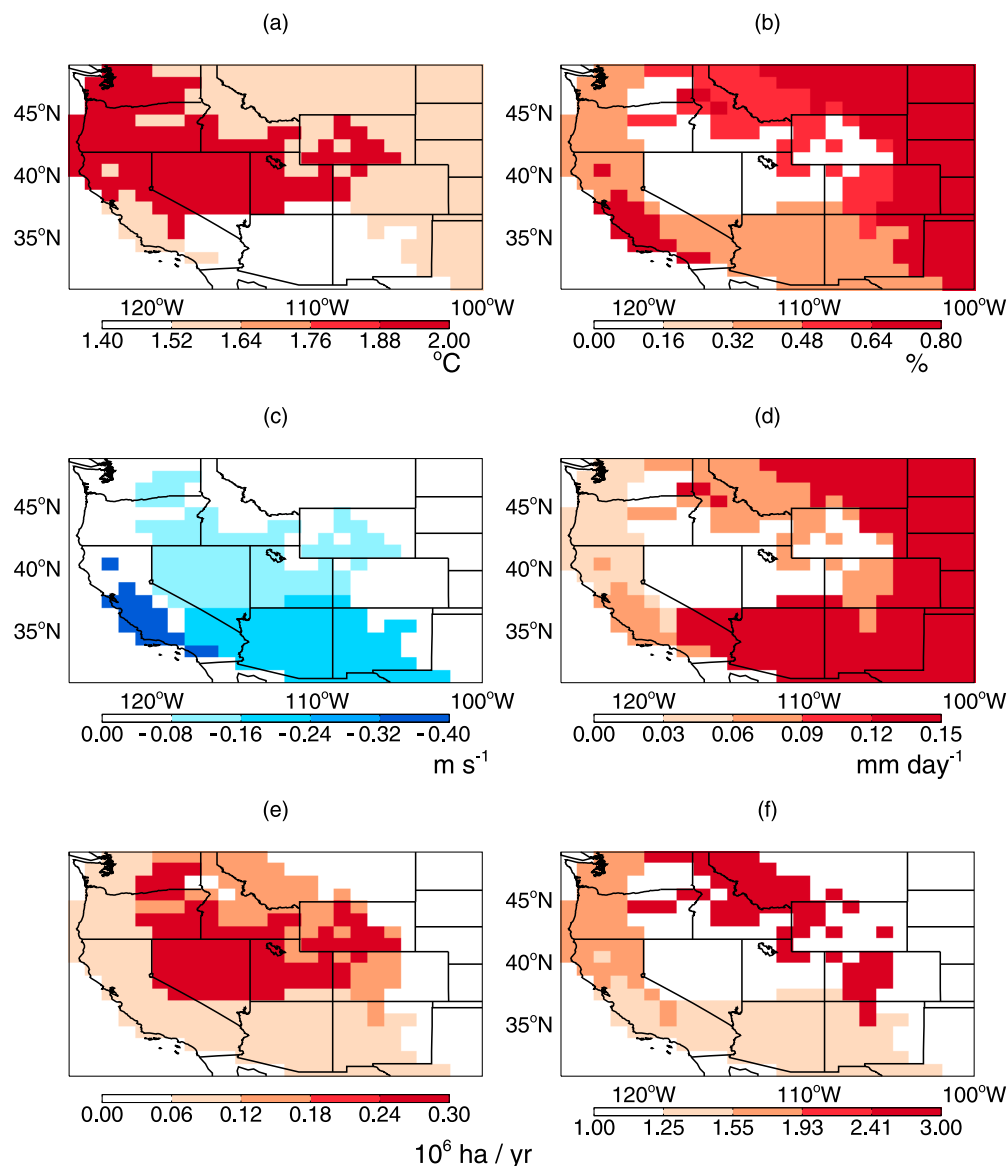


Figure 5. Simulated 1996–2055 change in May–October local noon meteorology from the GISS GCM and IPCC A1B emissions scenario. Values are the difference between 10-year means for 2046–2055 and 1996–2005. (a) Surface temperature, (b) relative humidity, (c) wind speed, (d) 24-h accumulated rainfall. Also shown is the wildfire area burned predicted by our regression equations and GCM meteorology for (e) present day (1996–2005) and (f) ratio of predicted area burned 2046–2055:1996–2005.

than 2%, respectively, across the western United States with the greatest increases in the Eastern Rocky Mountains/Great Plains and Desert Southwest ecoregions. Mean wind speeds are projected to decrease slightly throughout the western United States. These climate projections lie within the range reported by the Intergovernmental Panel on Climate Change [Seager *et al.*, 2007; Christensen *et al.*, 2007], giving us confidence that the climate projections from the GISS model are robust.

[19] We applied the adjusted GCM meteorology to our area burned regression model to predict annual ecoregion area burned from 1996 to 2055. Table 2 shows the average observed area burned for 1980 to 2004 and average calculated area burned for a 10-year period in the present day (1996 to 2005) and in the future (2046 to 2055) for each of

the six ecoregions. Average area burned in the present day is calculated with a normalized mean bias ($NMB = 100\% \times \sum_{i=1}^N (P_i - O_i) / \sum_{i=1}^N O_i$, where P_i is the predicted area burned during year i and O_i is the observed area burned during year i and N is the number of years in the analysis) of +10% to –25% depending on the region. Figure 5e shows simulated annual area burned for 1996–2005, and Figure 5f shows the ratio of area burned in 2046–2055 to that in 1996–2005.

[20] Total area burned across the western United States is projected to increase by 54% for 2046–2055 relative to 1996–2005. This projected increase is significant (student's t test $p = 0.03$). Area burned is predicted to increase in all regions except the Eastern Rocky Mountains/Great Plains where the change is not significant. Statistically significant

Table 2. Annual Mean Observed (1980–2004) and Simulated Area Burned $\pm 1\sigma$ by Ecoregion in the Western United States^a

| Ecoregion | Area Burned/10 ⁵ ha | | | | | Standardized Departure ^b | Slope ^c $\pm 1\sigma$ (ha/yr) | p Value for Slope |
|--------------------------------------|--------------------------------|-----------------|-----------------|----------------|----------------|-------------------------------------|--|-------------------|
| | Observed | | Predicted | | | | | |
| | 1980–2004 | 1996–2005 (PD) | 2046–2055 (F) | Ratio (F)/(PD) | Ratio (F)/(PD) | | | |
| Pacific Northwest | 1.08 \pm 0.39 | 1.08 \pm 0.70 | 1.92 \pm 0.79 | 1.78 | 1.78 | 1.23 | 1440 \pm 470 | <0.01 |
| California Coastal Shrub | 0.59 \pm 0.17 | 0.60 \pm 0.43 | 0.84 \pm 0.31 | 1.38 | 1.38 | 0.61 | 320 \pm 310 | 0.15 |
| Desert Southwest | 0.74 \pm 0.14 | 0.81 \pm 0.22 | 1.16 \pm 0.18 | 1.43 | 1.43 | 1.42 | 690 \pm 160 | <0.01 |
| Nevada Mountains/Semidesert | 2.84 \pm 0.71 | 3.04 \pm 1.03 | 3.14 \pm 0.67 | 1.03 | 1.03 | 0.13 | -140 \pm 590 | 0.41 |
| Rocky Mountains Forest | 2.07 \pm 0.71 | 1.53 \pm 1.52 | 4.19 \pm 1.76 | 2.75 | 2.75 | 1.44 | 5010 \pm 1220 | <0.01 |
| Eastern Rocky Mountains/Great Plains | 0.78 \pm 0.26 | 0.55 \pm 0.85 | 0.50 \pm 0.67 | 0.91 | 0.91 | -0.07 | -400 \pm 540 | 0.23 |

^aPD, Present Day; F, Future.

^bThe standardized departure is the absolute change [F-PD] divided by the standard deviation [$\sigma_{(1996-2055)}$] in predicted area burned.

^cThe trend in predicted area burned (1996–2055) is fitted using linear regression and the slope of the best fit line is reported.

($p < 0.05$) increases in area burned are projected for the Rocky Mountains Forest (78%), Pacific Northwest Forest (175%), and Desert Southwest (43%) ecoregions (see Table 2). In these ecoregions, area burned by mid-century is predicted to increase by more than one standard deviation. We used our regression equations (Table 1) along with the predicted changes in meteorological and FWI parameters to quantify the contributions of the different predictors to the change in predicted area burned (see Table 3). Simulated increases in temperature (Figure 5) are responsible for more than 80% of the predicted increase in area burned in these ecoregions.

[21] For most of the west, temperature plays the main role in driving future changes in area burned. However, the small (but insignificant) reduction in area burned in the Great Plains/Eastern Rocky Mountains is due to increased precipitation simulated by the GCM. In the Nevada Mountains/Semidesert and to a lesser extent in the Desert Southwest ecoregions the impact of increasing temperature is partly offset by increasing precipitation; there is no significant change in area burned in the former region and a 43% increase in the Desert Southwest ecoregion.

[22] Figure 6 shows the interannual variability in predicted area burned and in the predictors used to calculate area burned in the Pacific Northwest and Rocky Mountains Forest ecoregions. Interannual variability in predicted area burned is similar to that in observed area burned. We fit the predicted trend in area burned for each ecoregion during the period 1980 to 2004 using linear regression and found that the Pacific Northwest, Desert Southwest, and Rocky Mountains Forest ecoregions have significant positive trends, as shown in Table 2.

2.3. Production of Wildfire Emissions

[23] To calculate emissions from wildfires, we took the following steps. We first converted annual area burned to monthly area burned by using the average observed seasonal variability of wildfire in each ecoregion in 1980–2004. We assumed that the seasonality of wildfire remains the same in the future and that the emissions of wildfires are constant across a month. Calculated ecoregion area burned was mapped onto a $1^\circ \times 1^\circ$ grid using the observed area burned data to constrain the typical spatial extent of fires within each ecoregion. Figure 7 shows the fraction of $1^\circ \times 1^\circ$ grid squares that contain 70% of observed annual area burned in any 1 year in each of the six ecoregions. We repeated this procedure for 60, 80, and 90% of area burned, but changing this had little impact on our results. For all ecoregions, 70% of area burned in a particular year occurs in 5–25% of the ecoregion. To match this observed behavior, we place 70% of projected area burned in 10% of $1^\circ \times 1^\circ$ grid squares in each ecoregion. We locate these grid squares randomly within each ecoregion. The remaining 30% of area burned was averaged across the remaining 90% of grid squares within the ecoregion. To check for bias introduced by the random placement of wildfires within each ecoregion, we created a 100-member ensemble of simulations of yearly biomass consumption, each with a different randomly chosen set of wildfire locations. Our results showed only a 1% one-sigma variation in total biomass consumption over the simulation period.

Table 3. Present-Day (1996–2005) and Future (2046–2055) May–October Values of Predictors Simulated Using the GISS GCM and FWI System and Used to Calculate Area Burned^a

| Ecoregion | Simulated Mean | | Standardized Departure ^b | <i>p</i> Value ^c | Percent Contribution ^d |
|-----------------------------|----------------|-----------|-------------------------------------|-----------------------------|-----------------------------------|
| | 1996–2005 | 2046–2055 | | | |
| Pacific Northwest | | | | | |
| DC | 595 | 605 | 0.2 | 0.7 | 10 |
| T/°C | 24.9 | 26.9 | 1.7 | <0.01 | 90 |
| Californian Coastal Shrub | | | | | |
| T _{max} /°C | 37.7 | 39.2 | 1.1 | <0.01 | 95 |
| FFMC | 90.4 | 90.5 | 0.1 | 0.90 | 5 |
| Desert Southwest | | | | | |
| T/°C | 26.5 | 27.9 | 1.7 | <0.01 | 108 |
| DC | 590 | 566 | −0.5 | 0.24 | −8 |
| Nevada Mountains/Semidesert | | | | | |
| FWI _{max} | 92.1 | 95.0 | 0.3 | 0.38 | 180 |
| Rain/mm/d | 0.54 | 0.56 | 0.1 | 0.85 | −80 |
| Rocky Mountains Forest | | | | | |
| T/°C | 18.8 | 20.4 | 1.8 | <0.01 | 80 |
| BUI _{max} | 153 | 176 | 0.6 | 0.23 | 20 |
| Great Plains | | | | | |
| DSR | 5.9 | 5.7 | −0.1 | 0.38 | 100 |

^aSee Table 1. Definition of predictors is in footnote of Table 1.

^bStandardized departure is the future minus present-day simulated means divided by the standard deviation for each predictor.

^cStudent's *t* test calculated from the difference between the present-day and future simulated means.

^dThe percentage contribution to the change in area burned is calculated for each predictor using the regressions in Table 1 and the change in predictor reported here.

[24] Fuel consumption was calculated from a detailed database of fuel loading (i.e., available fuel) for the United States developed by the U.S. Forest Service, the Fuel Characteristic Classification System (FCCS) (<http://www.fs.fed.us/pnw/fera/fccs/>), and the fraction of fuel load-

ing that is burned as a function of fire severity for different categories of fuel. We assume that fires burn with 25% high, 25% medium, and 25% low severity, and that 25% of the area is unburned, on the basis of an analysis of the largest wildfires in 2002 in the lower 48 states [Randall, 2004]. The

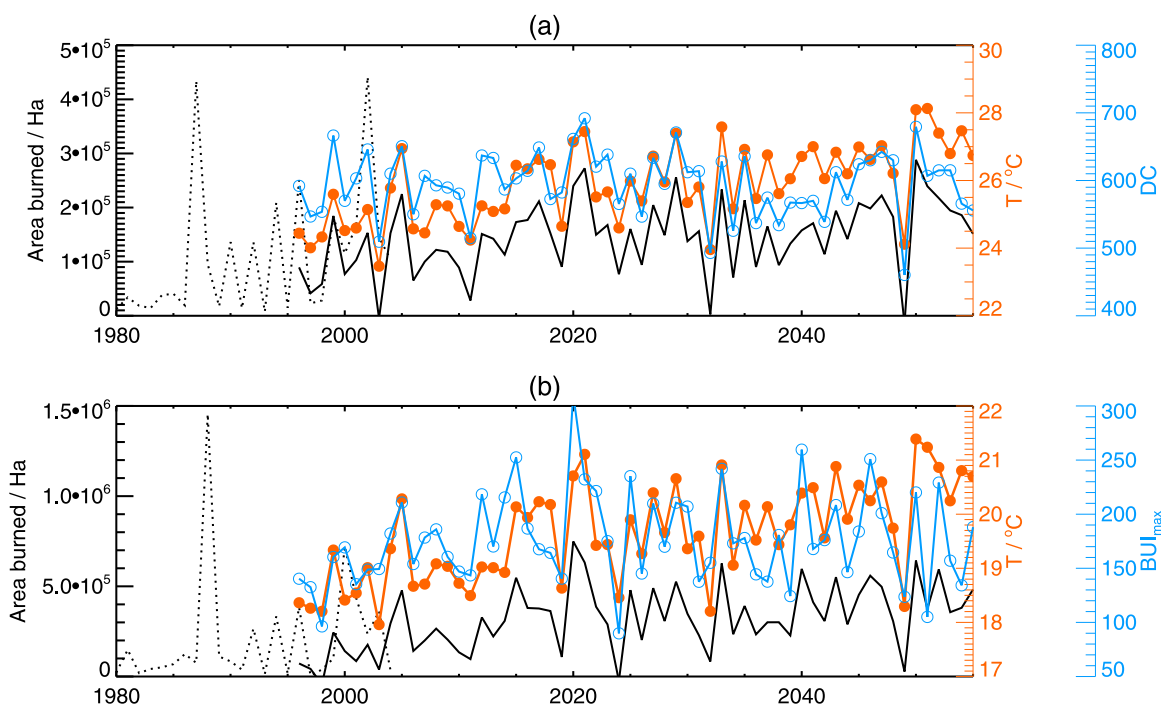


Figure 6. Annual area burned and May–October values of predictors used in regression equations for (a) Pacific Northwest and (b) Rocky Mountains Forest ecoregions between 1980 and 2055. Observed area burned (dotted black line) and predicted area burned (solid black line). Temperature (filled circles) and indices from the Canadian FWI System (see Figure 3, open circles) are calculated using the GISS GCM.

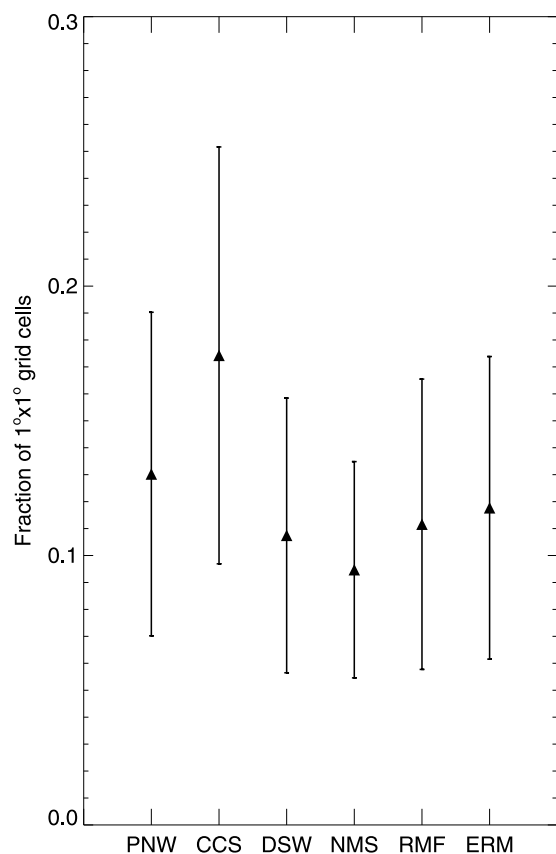


Figure 7. Fraction of $1^{\circ} \times 1^{\circ}$ grid squares (solid symbols show the mean and error bars one standard deviation) within each ecoregion that contain 70% of observed area burned in any year calculated for the period 1980–2004. Ecoregions are as follows: PNW, Pacific Northwest; CCS, Californian Coastal Shrub; DSW, Desert Southwest; NMS, Nevada Mountains/Semidesert; RMF, Rocky Mountains Forest and ERM, Eastern Rocky Mountains/Great Plains.

FCCS gives the fuel loadings for many fuel beds with resolution of $1 \text{ km} \times 1 \text{ km}$ [McKenzie *et al.*, 2007; Ottmar *et al.*, 2007; Riccardi *et al.*, 2007]. The loading for each fuel bed is given for various size categories of fuels that correspond to time-lag fuel categories commonly used in fire behavior modeling in the United States. Fuel consumption was calculated from fuel loadings by adopting the fraction of fuel that is burned in low-severity, medium-severity, and high-severity fires in six classes of fuel given in Table 4. The fractions in Table 4 are used by the U.S. Geological Survey to derive the severity of a burn using field observations of fractional consumption after the fire

(http://frames.nbii.gov/ffi/docs/Composite_Burn_Index.pdf). We matched the FCCS fuel categories to the fuel classes of the Composite Burn Index in Table 4 as follows: (1) litter/light fuels: FCCS categories of litter and woody fuels $<7.6 \text{ cm}$ in diameter, (2) medium fuel: FCCS woody fuels $7.6\text{--}20.3 \text{ cm}$ in diameter, and (3) heavy fuel: FCCS woody fuel $>20.3 \text{ cm}$ in diameter. Fuel consumption was calculated for each 1 km^2 grid, weighted by severity, and then an average formed for each $1^{\circ} \times 1^{\circ}$ grid, the resolution of our area burned product. Average fuel consumption is shown in Figure 8a.

[25] Emissions of carbonaceous aerosol from wildfires were calculated using the predicted $1^{\circ} \times 1^{\circ}$ wildfire area burned maps combined with the $1^{\circ} \times 1^{\circ}$ fuel consumption product and emission factors from *Andreae and Merlet* [2001]. We assume that fuel loadings and fire severity do not change between present day and 2050, so that the emissions of carbonaceous aerosol per unit area burned do not change over the simulation period. That is, the simulated change in wildfire emissions is driven solely by changes to wildfire area burned. A database of monthly biomass consumption on the $1^{\circ} \times 1^{\circ}$ grid is available on request.

[26] We find that wildfires in the Pacific Northwest and Rocky Mountains Forest ecoregions dominate present-day biomass consumption by fires in the western United States, accounting for 30 and 43%, respectively, of the total consumption for 1980–2004 using the observed area burned from *Westerling et al.* [2003] with updates (see Table 5). Wildfire in these two ecoregions will therefore have the largest potential impact on regional air quality. The Nevada Mountains/Semidesert ecoregion has the greatest area burned, 35% of the total for 1980–2004 (Table 2), but accounts for only 7% of the total biomass consumption because of low fuel loads. Similarly, the Californian Coastal Shrub and Desert Southwest with 16% of area burned account for only 6% of total biomass consumption. Figures 8b and 8c contrast the different spatial distributions of area burned and fuel consumption in the western United States.

[27] The calculated annual mean dry biomass consumption based on observed area burned is 14.2 Tg for 1980–2004. Predicted mean dry biomass consumption in the western United States, averaged over the 100-member ensemble of simulations, increases from $\sim 13.8 \text{ Tg/a}$ for 1996–2005 to $\sim 26.4 \text{ Tg/a}$ for 2046–2055, an increase of $\sim 90\%$ (see Table 5). This increase is statistically significant ($p < 0.01$). The linear trend in biomass consumption is $0.23 \pm 0.07 \text{ Tg/yr}$. Figure 9 shows the trend in predicted dry biomass consumption by wildfire in the western United States for 1996–2055 plotted as the standardized departure from the mean for 1996–2005 (Standardized departure_{*i*} = $[P_i - \bar{P}_{(1996-2005)}]/\text{standard deviation}(P_{1996-2005})$,

Table 4. Fractional Fuel Consumption as a Function of Fire Severity

| Burn Severity | Litter and Light Fuels ^a | Medium Fuels ^b | Heavy Fuels ^c | Duff ^d | Grass | Shrub | Canopy |
|---------------|-------------------------------------|---------------------------|--------------------------|-------------------|-------|-------|--------|
| Low | 0.5 | 0.2 | 0.1 | 0.0 | 0.3 | 0.2 | 0.05 |
| Medium | 1.0 | 0.4 | 0.25 | 0.5 | 0.8 | 0.7 | 0.5 |
| High | 1.0 | 0.6 | 0.4 | 1.0 | 1.0 | 1.0 | 0.95 |

^aWoody fuels $<7.6 \text{ cm}$ in diameter.

^bWoody fuels $7.6\text{--}20.3 \text{ cm}$ in diameter.

^cWoody fuels $>20.3 \text{ cm}$ in diameter.

^dDepth of duff was converted to fuel loading in western forest ecosystems using a density of $1.63 \text{ kg/m}^2/\text{cm}$ depth [van Wageningen *et al.*, 1998].

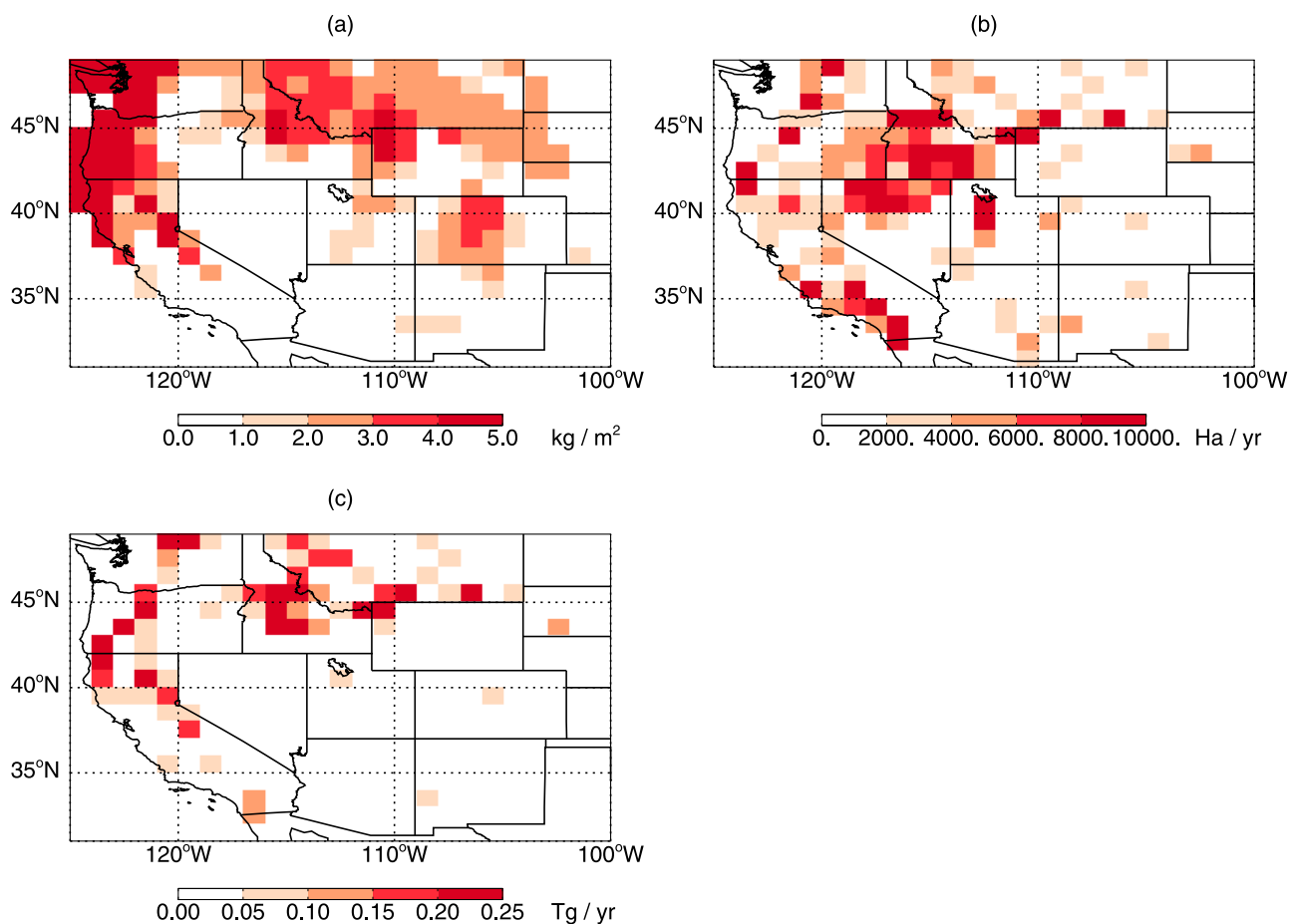


Figure 8. (a) Mean dry biomass consumption per unit area burned (see section 2.3 for details) and annual mean (b) observed area burned [Westerling *et al.*, 2003] and (c) dry biomass consumption for the period 1980–2004. Color scale saturates at respective values.

where P_i is the biomass consumption in year i). A low fire year in 2046–2055 (except for 2049) is about one standard deviation above the 1996–2005 mean and is equivalent to a high fire year during 1996–2005.

[28] The projected increase in future area burned may result in a decrease in the fire return interval, and thus a decrease in the average stand age and in the mean fuel load, with implications for our projected future emissions from wildfires. A maximum reduction in fuel burned can be estimated by assuming that there is no recovery of vegetation after a wildfire; that is, the fuel loading is zero if the same area reburns, with random placement of fires within each ecozone each year. When we make this assumption our projected biomass consumption in the western United States in 2046–2055 is 18% less than when we assume constant fuel consumption. This is obviously an unrealistic scenario but gives a plausible estimate of the maximum reduction in fuel consumption caused by an increase in area burned over 50 years. For the rest of this work we assume that fuel loads do not vary over the simulation period.

3. Simulations of Atmospheric EC and OC

[29] We use our simulated wildfire emissions along with a global chemistry model to calculate the changes in aerosol air quality over the western United States.

3.1. Model Description

[30] We predict atmospheric carbonaceous aerosol concentrations using the GEOS-Chem global 3-D model of tropospheric chemistry [Bey *et al.*, 2001; Park *et al.*, 2003] driven by meteorological fields from the NASA/GISS GCM. The interface between the GEOS-Chem CTM and the GISS GCM is described by Wu *et al.* [2007, 2008] and validated for gas phase species by Wu *et al.* [2007] and for aerosols by Liao *et al.* [2007]. We described the GISS model version used in this work in section 2.2.

[31] Meteorological output from the GISS GCM was archived with 6-h resolution (3 h for surface quantities and mixing depths) and used as input to the CTM. We used GEOS-Chem model version v7.04.01 (see <http://www-as.harvard.edu/chemistry/trop/geos>) with the same spatial resolution as the GCM, $4^\circ \times 5^\circ$.

[32] The model treats EC and OC with a hydrophobic and hydrophilic fraction for each (giving four advected tracers). Combustion sources emit hydrophobic aerosol which become hydrophilic with an e-folding time of 1.2 days [Cooke *et al.*, 1999; Chin *et al.*, 2002]. We assumed that 80% of EC and 50% of OC emitted from primary sources are hydrophobic [Cooke *et al.*, 1999; Chin *et al.*, 2002; Chung and Seinfeld, 2002]. Anthropogenic emissions of OC over the United States are from Cooke *et al.* [1999] with the

Table 5. Annual Mean Dry Biomass Consumption by Wildfire in the Western United States

| Ecoregion | Annual Mean Biomass Consumption/Tg | | | |
|--------------------------------------|------------------------------------|-----------|-----------|-----------------------------|
| | Observed 1980–2004 | Simulated | | <i>p</i> Value ^a |
| | | 1996–2005 | 2046–2055 | |
| Pacific Northwest | 4.23 | 6.33 | 11.31 | 0.04 |
| California Coastal Shrub | 0.46 | 0.61 | 0.82 | 0.36 |
| Desert Southwest | 0.39 | 0.30 | 0.42 | 0.05 |
| Nevada Mountains/Semidesert | 1.02 | 1.43 | 1.48 | 0.66 |
| Rocky Mountains Forest | 6.06 | 4.19 | 11.51 | <0.01 |
| Eastern Rocky Mountains/Great Plains | 2.07 | 0.97 | 0.88 | 0.88 |
| Western U.S. Total | 14.2 | 13.8 | 26.4 | 0.01 |

^aStudent's *t* test *p* value calculated from the difference between the present-day and future simulated means.

correction factor from *Park et al.* [2003]. Biofuel OC emissions are from *Yevich and Logan* [2003] and from *Park et al.* [2003] for the United States. In the western United States, we used fire emissions calculated as described in section 2.3, using one member of the ensemble of simulations with random placement of fires within each ecoregion. Outside of the western United States we used climatological biomass burning emissions derived from *Loberth et al.* [1999] with seasonality from *Duncan et al.* [2003]. We assumed that wildfire emissions are constant across each month. Biomass burning emissions were emitted into the boundary layer. The model includes secondary organic aerosol (SOA) formation from biogenic terpenes. Emissions of monoterpenes were calculated using *Guenther et al.* [1995] and vary according to temperature and solar radiation. We did not account for the effects of changing CO₂ concentrations on vegetation [e.g., *Constable et al.*, 1999] or changing land cover [*Sanderson et al.*, 2003] on biogenic monoterpene emissions. We assumed a 10% carbon yield of hydrophilic OC from terpenes [*Chin et al.*, 2002]. We do not account for the formation of SOA from isoprene which over the western United States may contribute a similar amount of SOA to that from monoterpenes [*Liao et al.*, 2007]. A global evaluation of GEOS-Chem EC and OC is given by *Chin et al.* [2002], and a more detailed evaluation over the United States can be found in the work of *Park et al.* [2003].

3.2. Impact of Future Wildfires on Carbonaceous Aerosol Concentrations

[33] The short lifetime of EC and OC results in concentrations over the western United States being dominated by emissions from the United States. In the work of *Spracklen et al.* [2007] we showed that interannual variability in western United States wildfire emissions controls much of the observed interannual variability in summertime atmospheric OC concentrations. *Park et al.* [2003] showed that trans-Pacific transport from natural and anthropogenic Asian sources contributes only 2% of the United States OC burden. Here we make a first prediction of the impacts of climate change on future carbonaceous aerosol concentrations in the western United States resulting from a change in the area of western United States fires, assuming that wildfires outside the western United States remain constant. To isolate the impacts of changes in fires resulting from changes in climate, we maintained anthropogenic emissions of EC and OC from fossil fuel and biofuel sources at their present-day values.

[34] We performed two 5-year simulations for the present day (1996–2000) and for the mid-21st century (2046–2050). Each model run was initialized with a 1-year spin-up. Figure 10 shows simulated summertime OC and EC concentrations in the western United States for these two time periods. Summertime mean concentrations of OC over the western United States increase from 1.4 $\mu\text{g m}^{-3}$ to 2.1 $\mu\text{g m}^{-3}$ over 50 years (an increase of 40%) whereas EC increases from 0.18 $\mu\text{g m}^{-3}$ to 0.21 $\mu\text{g m}^{-3}$ (18%). The smaller fractional increase in EC concentrations is a result of EC in the western United States being more dominated by fossil fuel emissions than is OC [*Spracklen et al.*, 2007]. The maximum increase in carbonaceous aerosol concentrations occurs over the northwest United States (Oregon, Washington, Idaho, western Montana, and northern California, United States) where absolute OC increases 1–4 $\mu\text{g m}^{-3}$ (15–70%) and EC aerosol increases 0.05–0.2 $\mu\text{g m}^{-3}$ (10–70%). These large increases in carbonaceous aerosol are caused by the large increase in area burned simulated for the Pacific Northwest and Rocky Mountains Forest ecoregions (Table 2). The smaller increases in carbonaceous aerosol in the southwest (southern California, Arizona, and New Mexico) reflect the smaller predicted increases in wildfires in these areas.

[35] This projected change in aerosol concentrations is caused by a combination of different effects including changes in wildfire emissions, atmospheric transport, wet

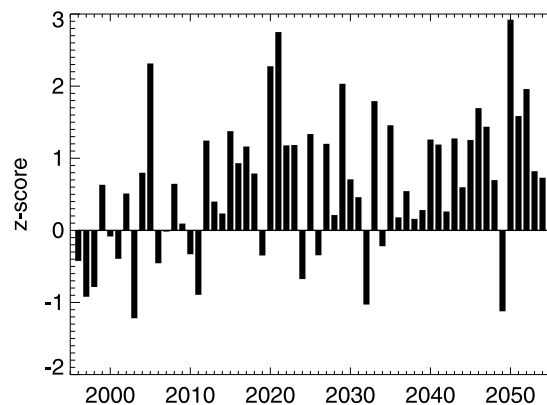


Figure 9. Predicted annual dry biomass consumption by wildfires in the western United States between 1996 and 2055 using meteorology from the GISS GCM combined with our wildfire regressions (see Table 1). We show results as a z score, or standardized departure (the number of standard deviations away from the 1996–2005 mean).

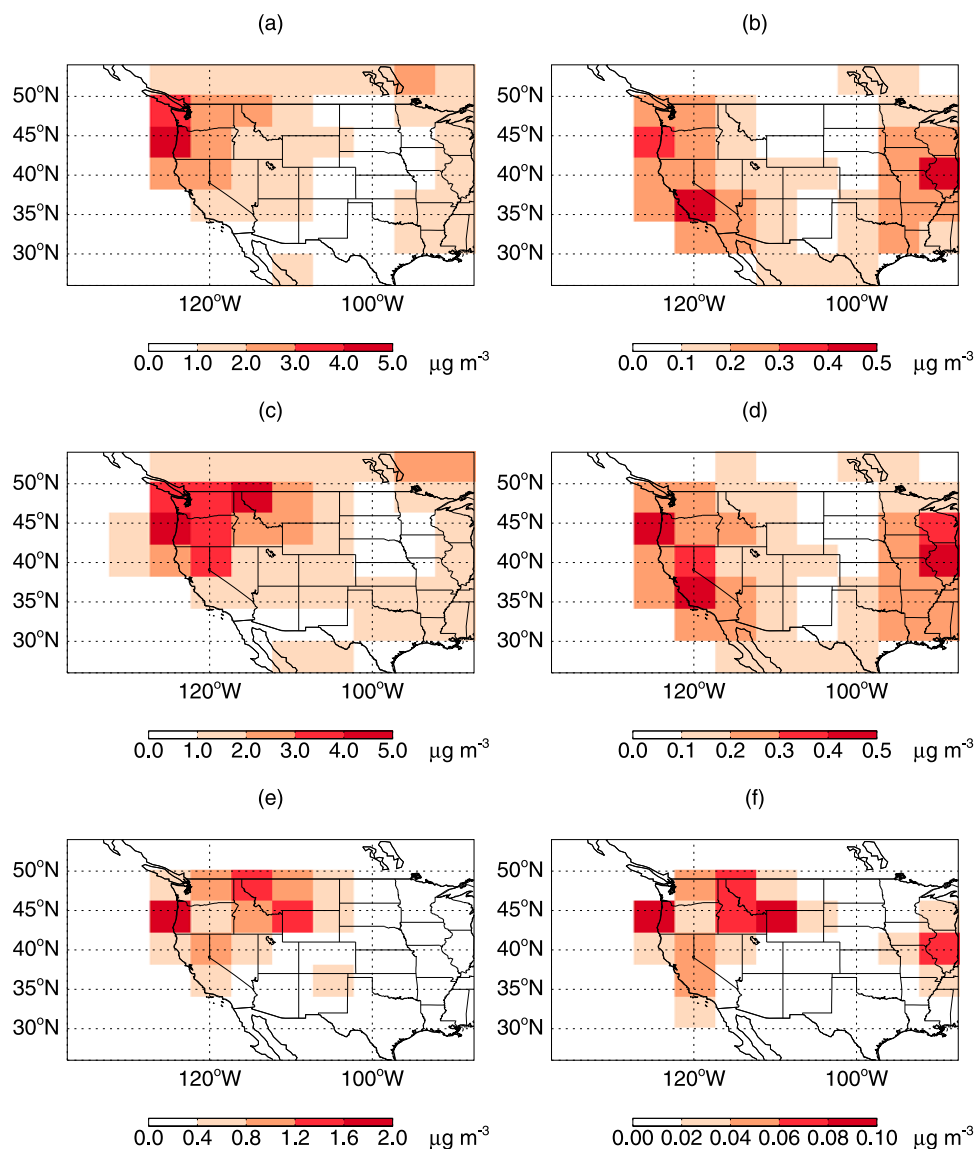


Figure 10. Simulated summertime (June–August) (left) mean surface OC and (right) EC aerosol concentrations over the western United States during (a and b) 1996–2000 and (c and d) 2046–2050. (e and f) The difference between simulated concentrations in 2046–2050 and 1996–2000. Units are $\mu\text{g m}^{-3}$.

and dry aerosol deposition, and biogenic emissions of monoterpenes which changes the amount of secondary organic aerosol (SOA). To evaluate the contribution of these different effects on future aerosol concentrations, we perform two additional simulations: one with future wildfires driven by climate change but where we maintain atmospheric transport, deposition, and monoterpene emissions at present-day values, and one with future atmospheric transport, deposition, and monoterpene emissions but where we maintain wildfires at present-day values. Figure 11 summarizes the results for the western United States (31–49°N, 125–100°W) for these scenarios and for the standard present-day and future simulations described in section 3.2. Interannual variability in weather is important as can be seen in the calculated aerosol concentrations: a cold future summer (year 4) shows up clearly as a year with low regionally averaged concentrations of both OC and EC

aerosol. As we saw above, a combination of changing atmospheric transport, deposition, wildfires, and monoterpene-derived SOA results in western United States EC concentrations (2046–2050) increasing by 18% and OC concentrations increasing by 40% relative to 1996–2000. In the model simulations where we increase wildfire emissions but keep atmospheric transport, aerosol deposition, and monoterpene emissions constant (future fires and PD climate) we calculate that EC concentrations increase by 17% and OC concentrations increase by 30%. Increased wildfire emissions caused by changing climate therefore dominate our projected future change in carbonaceous aerosols, resulting in 75% of the change in OC and 95% of the change in EC concentrations.

[36] Simulated EC concentrations with future atmospheric transport, deposition, and monoterpene emissions but with present-day wildfire emissions (PD fires and future climate)

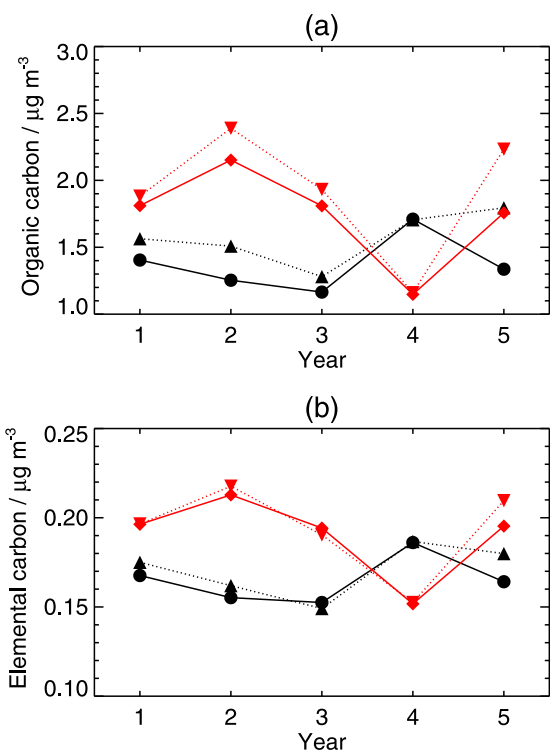


Figure 11. Simulated summertime average (June–August) surface concentrations of (a) OC and (b) EC in the western United States (31° – 49° N, 125° – 100° W) for (1) present-day wildfires (1996–2000) and present-day climate (circles), (2) present-day wildfires but with future (2046–2050) climate (upward triangles), (3) future wildfires but with present-day climate (diamonds), and (4) future wildfires and future climate (downward triangles).

increase by only 3%. Using the same GISS model, *Wu et al.* [2008] calculated a 5% decrease in afternoon mixing depths over the northwest in the future climate, which would increase EC concentrations. However, this effect is offset by increasing precipitation in this region which will increase aerosol wet deposition and reduce EC concentrations. Concentrations of OC in the future climate, but with present-day wildfires, are 14% greater than present day. Most of this change (80%) is caused by increasing temperature driving increased monoterpene emissions and SOA formation, with the remainder caused by changing atmospheric transport and aerosol deposition. The temperatures projected by the GISS model combined with the *Guenther et al.* [1995] biogenic emissions algorithm predict a 20% increase in monoterpene emissions in the United States by 2050. Biogenic emissions of isoprene may also change in the future resulting in an additional change to SOA that is not considered here. However, the projected future change in isoprene emissions is currently uncertain [*Heald et al.*, 2009].

4. Discussion and Conclusions

[37] We have quantified for the first time the effect of changing wildfire activity in a warming climate on carbonaceous aerosol concentrations in the western United

States in future decades. We used stepwise linear regression to derive relationships between observed meteorology and observed wildfire area burned for 1980–2004. Our regressions are ecosystem dependent, with temperature and fuel moisture explaining 24–57% of the variance in annual area burned. Our focus is on the prediction of wildfire in forest dominated ecosystems that contribute most substantially to carbonaceous aerosol emissions because of their greater fuel loads. Our approach works well for these ecosystems where the meteorology of the particular fire season has the dominant control on fire, but less well for shrub and grass dominated ecosystems where fuel loads, and hence wildfire, is strongly influenced by the previous year's precipitation [*Littell et al.*, 2009].

[38] Following the IPCC A1B greenhouse gas scenario, the GISS GCM predicts a 2 K increase in summertime temperature and a $\sim 7\%$ increase in summertime precipitation by midcentury in the western United States. These predicted changes in climate increase projected area burned in the western United States in 2046–2055 by 54% relative to 1996–2005. Predicted changes to area burned vary regionally, from no change to an increase of 175%, because of regional changes in simulated climate combined with varying ecosystem response to a changing climate. The largest increases in area burned are projected for the Pacific Northwest (78%) and Rocky Mountains Forest (175%) ecoregions where wildfire appears to depend most strongly on temperature. This is consistent with the change in wildfire activity observed in the western United States over the past few decades; sixty percent of the observed increase in large (>400 ha) forest fire area burned that occurred between 1970–1986 and 1987–2003 was located in the northern Rockies, and 18% in the Sierra Nevada, Cascades, and coast ranges of Oregon and California [*Westerling et al.*, 2006]. Our method projects little change in area burned by 2050 for the Nevada Mountains/Semidesert and Eastern Rocky Mountains/Great Plains ecoregions because simulated increases in precipitation compensate for increases in temperature in these regions.

[39] We use the GEOS-Chem CTM, driven by meteorology from the GISS GCM, to predict changes in carbonaceous aerosol concentrations over the western United States. We predict that mean summertime OC concentrations in 2046–2050 increase by 40% (from 1.5 to 2.1 $\mu\text{g m}^{-3}$), and EC concentrations increase by 18% (from 0.18 to 0.22 $\mu\text{g m}^{-3}$) relative to 1996–2000. The largest projected increases are in the northwest United States, collocated with the greatest increases in wildfire. Most of the increase in carbonaceous aerosol concentrations (95% for EC and 75% for OC) is caused by increases in wildfire emissions, which are predicted to increase by 90%. Changes in meteorology that occur between present day and midcentury contribute about 5–10% of the predicted change in carbonaceous aerosol concentrations. For OC, the remainder of the change (20%) is caused by the predicted increase in monoterpene emissions, due to rising temperature, and the resulting increase in secondary organic aerosol formation which has been previously predicted [*Heald et al.*, 2008].

[40] In common with previous studies of future wildfires, there are limitations in this study. We did not account for changes to vegetation, ignition, the length of fire season, or human activity on future area burned. Future wildfires may

be modified by changes in the distribution of vegetation caused either by direct anthropogenic land-use change or by climate change. In this paper, we considered a 50-year timescale over which vegetation will not change substantially, unless it is driven by wildfire [McKenzie *et al.*, 2004] or pest outbreaks [Logan *et al.*, 2003; Hicke *et al.*, 2006]. Changes to wildfire due to changes in lightning frequency [Price and Rind, 1994] and change to anthropogenic ignition [Wotton *et al.*, 2003] are also not considered here. A longer wildfire season is possible in a future climate, and an earlier start to the wildfire season has already been observed in the western United States [Westerling *et al.*, 2006]. We predict annual area burned and do not explore possible changes in the length of the fire season. Consequently, we focused on the air quality impact of wildfires in summer (June–August). This is the period of greatest wildfire activity and also the period when air quality degradation from wildfires is at its worst. However, longer wildfire seasons in the future may extend the negative impacts on air quality further into the spring and autumn.

[41] We assume that fuel consumption per unit area burned does not change over our simulation period. In reality, both fuel loads and fire severity may change, altering future fuel consumption. Increased wildfire area burned may drive reduced fire return intervals, vegetation stand age, and fuel consumption per unit area burned [Fellows and Goulden, 2008]. We estimated the maximum reduction in fuel consumption this effect can have by assuming no recovery of vegetation after a wildfire, such that areas that reburn over the period 1996–2055 result in no fuel consumption. With this assumption we calculate that biomass consumption in the western United States in 2046–2055 is 18% less than when we assume constant fuel consumption. Changes in vegetation caused by climate change, anthropogenic activity, or pest outbreaks will further affect fuel loads. Fuel consumption is also impacted by potential changes in fire severity. Climate change (increased temperature and wind speeds and reduced fuel moisture) may drive increases in fire severity, and hence increases in biomass consumption per unit area. A recent study has made the first projections of future wildfire emissions accounting for both changes in area burned and fire severity. Amiro *et al.* [2009] find that changes in wildfire biomass consumption from forest floor fuels in the Canadian boreal forest region are dominated by changes in area burned which are projected to increase by 93% under a $3 \times \text{CO}_2$ scenario. Under the same scenario, changes in fire severity are projected to increase biomass consumption by 0–18%, depending on the ecosystem. The impact of changing climate on fire severity in the western United States, where the forest types differ from those studied by Amiro *et al.* [2009], is currently not known. These combined changes in fuel loads and fire severity will likely have important impacts on future biomass consumption, either amplifying or suppressing the projected change in wildfire emissions calculated in this work.

[42] The vertical extent of wildfire emissions is a further uncertainty in our projected future aerosol concentrations. There is evidence that some fraction of wildfire emissions are injected above the boundary layer [Leung *et al.*, 2007; Mazzoni *et al.*, 2007; Kahn *et al.*, 2007]. How this injection height will vary in the future with potential changes in fire

severity and changes in atmospheric stability is also uncertain. In this study we have assumed wildfire emissions are injected into the boundary layer, and we do not consider any future change.

[43] This study has explored the role of future climate change on wildfire in the western United States. In this work we have evaluated the impacts of future climate change on wildfire area burned and carbonaceous aerosol concentrations over the western United States. We have not been able to account for the full set of variables and processes which are likely to control future wildfire emissions. In particular, future studies need to account for potential changes in vegetation, fuel loading (within the same vegetation type), fire severity, and fire ignition under a changing climate. In addition, it is important to explore the potential uncertainty associated with climate model projections, anthropogenic greenhouse gas emission scenarios, and fire prediction tools. Our predicted increase in wildfire has potential implications for ecology, carbon balance, land management, and fire suppression in western forests. In this work we focussed on the impacts of changing wildfire on carbonaceous aerosol concentrations. We predict summertime mean OC concentrations across the western United States to increase by 40% and EC concentrations to increase by 20% by midcentury relative to present day. This increase will have negative impacts on atmospheric visibility and human health. Carbonaceous aerosol currently accounts for 40% of fine aerosol mass in the western United States [Malm *et al.*, 2004]. Assuming other aerosol components remain unchanged, carbonaceous aerosol will account for ~50% of fine aerosol mass by midcentury. Future work is required to extend this study to the boreal forests of North America and Siberia, expand the impact to other atmospheric species such as ozone, and to study the potential climate feedbacks of increased wildfire [Randerson *et al.*, 2006].

[44] **Acknowledgments.** This work was funded by the National Aeronautics and Space Administration (NASA-MAP grant NNG06GB48G) and STAR Research Assistance agreement RD-83227501-0 awarded by the U.S. Environmental Protection Agency (EPA). This publication has not been formally reviewed by the EPA. The views expressed in this document are solely those of the authors, and the EPA does not endorse any products or commercial services mentioned in this publication.

References

- Allen, C., M. Savage, D. Falk, K. Suckling, T. Swetnam, T. Schulke, P. Stacey, P. Morgan, M. Hoffman, and J. Klingel (2002), Ecological restoration of southwestern ponderosa pine ecosystems: A broad perspective, *Ecol. Appl.*, *12*(5), 1418–1433.
- Amiro, B. D., A. Cantin, M. D. Flannigan, and W. de Groot (2009), Future emissions from Canadian boreal forest fires, *Can. J. For. Res.*, *39*, 383–395.
- Andreae, M., and P. Merlet (2001), Emission of trace gases and aerosols from biomass burning, *Global Biogeochem. Cycles*, *15*, 955–956.
- Bailey, R., P. Avers, T. King, and W. McNab (1994), Ecoregions and sub-regions of the United States (map), technical report, USDA For. Serv., Washington, D. C.
- Balling, R., G. Meyer, and S. Wells (1992), Relation of surface climate and burned area in Yellowstone National Park, *Agricul. For. Meteorol.*, *60*(3–4), 285–293.
- Bergeron, Y.-P., and M. Flannigan (1995), Predicting the effects of climate change on fire frequency in the southeastern Canada boreal forest, *Water Air Soil Pollut.*, *82*, 437–444.
- Bey, I., D. Jacob, R. Yantosca, J. Logan, B. Field, A. Fiore, Q. Li, H. Liu, L. Mickley, and M. Schultz (2001), Global modeling of tropospheric chemistry with assimilated meteorology: Model description and evaluation, *J. Geophys. Res.*, *106*, 23,073–23,096.

- Brown, T., B. Hall, and A. Westerling (2004), The impact of twenty-first century climate change on wildland fire danger in the western United States: An applications perspective, *Clim. Change*, 62(1–3), 365–388.
- Chin, M., P. Ginoux, S. Kinne, O. Torres, B. Holben, B. Duncan, R. Martin, J. Logan, A. Higurashi, and T. Nakajima (2002), Tropospheric aerosol optical thickness from the GOCART model and comparisons with satellite and sunphotometer measurements, *J. Atmos. Sci.*, 59, 461–483.
- Christensen, J., et al. (2007), Regional climate projections, in *Climate Change 2007: The Physical Science Basis. Contribution of Working Group I to the Fourth Assessment Report of the Intergovernmental Panel on Climate Change*, edited by S. Solomon et al., pp. 890–891, Cambridge Univ. Press, Cambridge, U. K.
- Chung, S., and J. Seinfeld (2002), Global distribution and climate forcing of carbonaceous aerosols, *J. Geophys. Res.*, 107(D19), 4407, doi:10.1029/2001JD001397.
- Constable, J., A. Guenther, D. Schimel, and R. Monson (1999), Modeling changes in VOC emission in response to climate change in the continental United States, *Global Change Biol.*, 5, 791–806.
- Cooke, W., C. Lioussé, H. Cachier, and J. Feichter (1999), Construction of a $1^\circ \times 1^\circ$ fossil fuel emission data set for carbonaceous aerosol and implementation and radiative impact in the ECHAM-4 model, *J. Geophys. Res.*, 104, 22,137–22,162.
- deBell, L., R. Talbot, J. Dibb, J. Munger, E. Fischer, and S. Frolking (2004), A major regional air pollution event in the northeastern United States caused by extensive forest fires in Quebec, *J. Geophys. Res.*, 109, D19305, doi:10.1029/2004JD004840.
- Duck, T., et al. (2007), Transport of forest fire emissions from Alaska and the Yukon Territory to Nova Scotia during summer 2004, *J. Geophys. Res.*, 112, D10S44, doi:10.1029/2006JD007716.
- Duffy, P., J. Walsh, J. Graham, D. Mann, and T. Rupp (2005), Impacts of large-scale atmospheric-ocean variability on Alaskan fire season severity, *Ecol. Appl.*, 15(4), 1317–1330.
- Duncan, B., R. Martin, A. Staudt, R. Yevich, and J. Logan (2003), Interannual and seasonal variability of biomass burning emissions constrained by satellite observations, *J. Geophys. Res.*, 108(D2), 4100, doi:10.1029/2002JD002378.
- Fellows, A., and M. Goulden (2008), Has fire suppression increased the amount of carbon stored in western U.S. forests?, *Geophys. Res. Lett.*, 35, L12404, doi:10.1029/2008GL033965.
- Flannigan, M., and C. Van Wagner (1991), Climate change and wildfire in Canada, *Can. J. For. Res.*, 21(1), 66–72.
- Flannigan, M., B. Stocks, and B. Wotton (2000), Climate change and forest fires, *Sci. Total Environ.*, 262(3), 221–229.
- Flannigan, M., I. Campbell, M. Wotton, C. Carcaillet, P. Richard, and Y. Bergeron (2001), Future fire in Canada's boreal forest: Paleocology results and general circulation model: Regional climate model simulations, *Can. J. For. Res.*, 31(5), 854–864.
- Flannigan, M., K. Logan, B. Amiro, W. Skinner, and B. Stocks (2005), Future area burned in Canada, *Clim. Change*, 72(1–2), 1–16.
- Gedalof, Z., D. Peterson, and N. Mantua (2005), Atmospheric, climatic, and ecological controls on extreme wildfire years in the northwestern United States, *Ecol. Appl.*, 15, 154–174.
- Gillett, N., A. Weaver, F. Zwiers, and M. Flannigan (2004), Detecting the effect of climate change on Canadian forest fires, *Geophys. Res. Lett.*, 31, L18211, doi:10.1029/2004GL020876.
- Girardin, M. (2007), Interannual to decadal changes in area burned in Canada from 1781 to 1982 and the relationship to Northern Hemisphere land temperatures, *Global Ecol. Biogeogr.*, 16(5), 557–566.
- Guenther, A., et al. (1995), A global model of natural volatile organic compound emission, *J. Geophys. Res.*, 100(D5), 8873–8892.
- Hansen, J., et al. (2002), Climate forcing in Goddard Institute for Space Studies S12000 simulations, *J. Geophys. Res.*, 107(D18), 4347, doi:10.1029/2001JD001143.
- Heald, C., et al. (2008), Predicted change in global secondary organic aerosol concentrations in response to future climate, emissions, and land use change, *J. Geophys. Res.*, 113, D05211, doi:10.1029/2007JD009092.
- Heald, C. L., M. J. Wilkinson, R. K. Monson, C. A. Alo, G. Wang, and A. Guenther (2009), Response of isoprene emission to ambient CO₂ changes and implications for global budgets, *Global Change Biol.*, 15(4), 1127–1140.
- Hicke, J., J. Logan, J. Powell, and D. Ojima (2006), Changing temperatures influence suitability for modeled mountain pine beetle (*Dendroctonus ponderosae*) outbreaks in the western United States, *J. Geophys. Res.*, 111, G02019, doi:10.1029/2005JG000101.
- Hodzic, A., S. Madronich, S. Massie, L. Menut, and C. Wiedinmyer (2007), Wildfire particulate matter in Europe during summer 2003: Meso-scale modeling of smoke emissions, transport and radiative effects, *Atmos. Chem. Phys.*, 7, 4043–4064.
- Houghton, J. (Ed.) (2001), *Climate Change 2001: The Scientific Basis*, Cambridge Univ. Press, Cambridge, U. K.
- Jaffe, D., I. Bertschi, L. Jaeglé, P. Novelli, J. Reid, H. Tanimoto, R. Vingarzan, and D. Westphal (2004), Long-range transport of Siberian biomass burning emissions and impact on surface ozone in western North America, *Geophys. Res. Lett.*, 31, L16106, doi:10.1029/2004GL020093.
- Jaffe, D., D. Chand, W. Hafner, A. Westerling, and D. Spracklen (2008a), Influence of fires on O₃ Concentrations in the western U.S., *Environ. Sci. Technol.*, 42(16), 5885–5891.
- Jaffe, D., W. Hafner, D. Chand, A. Westerling, and D. Spracklen (2008b), Interannual variations in PM_{2.5} due to wildfires in the western United States, *Environ. Sci. Technol.*, 42(8), 2812–2818.
- Kahn, R., W.-H. Li, C. Moroney, D. Diner, J. Martonchik, and E. Fishbein (2007), Aerosol source plume physical characteristics from space-based multiangle imaging, *J. Geophys. Res.*, 112, D11205, doi:10.1029/2006JD007647.
- Kasischke, E., and M. Turetsky (2006), Recent changes in the fire regime across the North American boreal region: Spatial and temporal patterns of burning across Canada and Alaska, *Geophys. Res. Lett.*, 33, L09703, doi:10.1029/2006GL025677.
- Lapina, K., R. Honrath, R. Owen, M. Martin, and G. Pfister (2006), Evidence of significant large-scale impacts of boreal fires on ozone levels in the midlatitude Northern Hemisphere free troposphere, *Geophys. Res. Lett.*, 33, L10815, doi:10.1029/2006GL025878.
- Leung, F.-Y., J. Logan, R. Park, E. Hyer, E. Kasischke, D. Streets, and L. Yurganov (2007), Impacts of enhanced biomass burning in the boreal forests in 1998 on tropospheric chemistry and the sensitivity of model results to the injection height of emissions, *J. Geophys. Res.*, 112, D10313, doi:10.1029/2006JD008132.
- Lewis, A., et al. (2007), Chemical composition observed over the mid-Atlantic and the detection of pollution signatures far from source regions, *J. Geophys. Res.*, 112, D10S39, doi:10.1029/2006JD007584.
- Liao, H., D. Henze, J. Seinfeld, S. Wu, and L. Mickley (2007), Biogenic secondary organic aerosol over the United States: Comparison of climatological simulations with observations, *J. Geophys. Res.*, 112, D06201, doi:10.1029/2006JD007813.
- Littell, J. S., D. McKenzie, D. L. Peterson, and A. L. Westerling (2009), Climate and ecoprovince fire area burned in western U.S. ecoprovinces, 1916–2003, *Ecol. Appl.*, 19(4), 1003–1021.
- Lobert, J., W. Keene, J. Logan, and R. Yevich (1999), Global chlorine emissions from biomass burning: The reactive chlorine emissions inventory, *J. Geophys. Res.*, 104, 8373–8390.
- Logan, J., J. Regniere, and J. Powell (2003), Assessing the impacts of global warming on forest pest dynamics, *Frontiers Ecol. Environ.*, 1(3), 130–137.
- Malm, W., B. Schichtel, M. Pitchford, L. Ashbaugh, and R. Eldred (2004), Spatial and monthly trends in speciated fine particle concentration in the United States, *J. Geophys. Res.*, 109, D03306, doi:10.1029/2003JD003739.
- Mazzoni, D., J. Logan, D. Diner, R. Kahn, L. Tong, and Q. Li (2007), A data-mining approach to associating MISR smoke plume heights with MODIS fire measurements, *Remote Sens. Environ.*, 107(1–2), 138–148.
- McKenzie, D., Z. Gedalof, D. Peterson, and P. Mote (2004), Climatic change, wildfire, and conservation, *Conserv. Biol.*, 18(4), 890–902.
- McKenzie, D., S. O'Neill, N. Larkin, and R. Norheim (2006), Integrating models to predict regional haze from wildland fire, *Ecol. Modell.*, 199, 278–288.
- McKenzie, D., C. Raymond, L.-K. Kellogg, R. Norheim, A. Andreu, A. Bayard, K. Kopper, and E. Elman (2007), Mapping fuels at multiple scales: landscape application of the Fuel Characteristic Classification System, *Can. J. For. Res.*, 37, 2421–2437.
- McMeeking, G., S. Kreidenweis, C. Carrico, T. Lee, J. Collett, and W. Malm (2005), Observations of smoke-influenced aerosol during the Yosemite Aerosol Characterization Study: Size distributions and chemical composition, *J. Geophys. Res.*, 110, D09206, doi:10.1029/2004JD005389.
- McMeeking, G., et al. (2006), Smoke-impacted regional haze in California during the summer of 2002, *Agricul. For. Meteorol.*, 137(1–2), 25–42.
- Moriondo, M., P. Good, R. Durao, M. Bindi, C. Giannakopoulos, and J. Corte-Real (2006), Potential impact of climate change on fire risk in the Mediterranean area, *Clim. Res.*, 31(1), 85–95.
- Noss, R., J. Franklin, W. Baker, T. Schoennagel, and P. Moyle (2006), Managing fire-prone forests in the western United States, *Frontiers Ecol. Environ.*, 4(9), 481–487.
- Ottmar, R., D. Sandberg, C. Riccardi, and S. Prichard (2007), An overview of the fuel characteristic classification system: Quantifying, classifying, and creating fuelbeds for resource planning, *Can. J. For. Res.*, 37(12), 2383–2393.
- Park, R., D. Jacob, M. Chin, and R. Martin (2003), Sources of carbonaceous aerosols over the United States and implications for natural visibility, *J. Geophys. Res.*, 108(D12), 4355, doi:10.1029/2002JD003190.

- Park, R., D. Jacob, and J. Logan (2007), Fire and biofuel contributions to annual mean aerosol mass concentrations in the United States, *Atmos. Environ.*, *41*, 7389–7400.
- Pfister, G., C. Wiedinmyer, and L. Emmons (2008), Impacts of the fall 2007 California wildfires on surface ozone: Integrating local observations with global model simulations, *Geophys. Res. Lett.*, *35*, L19814, doi:10.1029/2008GL034747.
- Price, C., and D. Rind (1994), The impact of a 2-X-CO₂ climate on lightning-caused fires, *J. Clim.*, *7*(10), 1484–1494.
- Randall, D. (2004), Strawman-approach for technical refinement of large fires and fire complexes for wrap phase 1 fire emissions inventory, *Tech. Rep. 178-6*, Air Sci. Inc., Portland, Or.
- Randerson, J., et al. (2006), The impact of boreal forest fire on climate warming, *Science*, *314*(5802), 1130–1132.
- Riccardi, C., R. Ottmar, D. Sandberg, A. Andreu, E. Elman, K. Kopper, and J. Long (2007), The fuelbed: A key element of the fuel characteristic classification system, *Can. J. For. Res.*, *37*(12), 2394–2412.
- Rind, D., J. Lerner, J. Jonas, and C. McLinden (2007), Effects of resolution and model physics on tracer transports in the NASA Goddard Institute for Space Studies general circulation models, *J. Geophys. Res.*, *112*, D05302, doi:10.1029/2006JD007801.
- Sanderson, M., C. Jones, W. Collins, C. Johnson, and R. Derwent (2003), Effect of climate change on isoprene emissions and surface ozone levels, *Geophys. Res. Lett.*, *30*(18), 1936, doi:10.1029/2003GL017642.
- Schmidt, G., et al. (2006), Present-day atmospheric simulations using GISS ModelE: Comparison to in-situ, satellite and reanalysis data, *J. Clim.*, *19*, doi:10.1175/JCLI3612.1.
- Seager, R., et al. (2007), Simulated changes in temperature are generally more consistent between different climate model simulations than changes in precipitation or wind speed, *Science*, *316*(1181), doi:10.1126/science.1139601.
- Skinner, W., B. Stocks, D. Martell, B. Bonsal, and A. Shabbar (1999), The association between circulation anomalies in the mid-troposphere and area burned by wildland fire in Canada, *Theoret. Appl. Climatol.*, *63*, 89–105.
- Skinner, W., A. Shabbar, M. Flannigan, and K. Logan (2006), Large forest fires in Canada and the relationship to global sea surface temperatures, *J. Geophys. Res.*, *111*, D14106, doi:10.1029/2005JD006738.
- Spracklen, D., J. Logan, L. Mickley, R. Park, R. Yevich, A. Westerling, and D. Jaffe (2007), Wildfires drive interannual variability of organic carbon aerosol in the western U.S. in summer, *Geophys. Res. Lett.*, *34*, L16816, doi:10.1029/2007GL030037.
- Stocks, B., et al. (1998), Climate change and forest fire potential in Russian and Canadian boreal forests, *Clim. Change*, *38*(1), 1–13.
- Stocks, B., et al. (2002), Large forest fires in Canada, 1959–1997, *J. Geophys. Res.*, *107*, 8149, doi:10.1029/2001JD000484, [printed 108(D1), 2003].
- Tymstra, C., M. Flannigan, O. Armitage, and K. Logan (2007), Impact of climate change on area burned in Alberta's boreal forest, *Int. J. Wildland Fire*, *16*(2), 153–160.
- Val Martin, M., R. Honrath, R. Owen, G. Pfister, P. Fialho, and F. Barate (2006), Significant enhancements of nitrogen oxides, black carbon, and ozone in the North Atlantic lower free troposphere resulting from North American boreal wildfires, *J. Geophys. Res.*, *111*, D23S60, doi:10.1029/2006JD007530.
- Van Wagner, C. (1987), The development and structure of the Canadian Forest Fire weather index system, *Tech. Rep. 35*, Can. For. Serv., Ottawa, Ont., Canada.
- van Wagtenonk, J., J. Benedict, and W. Sydoriak (1998), Fuel bed characteristics of Sierra Nevada conifers, *W. J. Appl. For.*, *13*, 73–84.
- Westerling, A., and B. Bryant (2008), Climate change and wildfire in California, *Clim. Change*, *87*, S231–S249.
- Westerling, A., A. Gershunov, D. Cayan, and T. Barnett (2002), Long lead statistical forecasts of area burned in western U.S. wildfires by ecosystem province, *Int. J. Wildland Fire*, *11*(3,4), 257–266.
- Westerling, A., A. Gershunov, T. Brown, D. Cayan, and M. Dettinger (2003), Climate and wildfire in the western United States, *Bull. Am. Meteorol. Soc.*, *84*(5), 595–604.
- Westerling, A., H. Hidalgo, D. Cayan, and T. Swetnam (2006), Warming and earlier spring increases western U.S. forest wildfire activity, *Science*, *313*(5789), 940–943.
- Wotowa, G., and M. Trainer (2000), The influence of Canadian forest fires on pollutant concentrations in the United States, *Science*, *288*, 324–328.
- Wotton, B., and M. Flannigan (1993), Length of the fire season in a changing climate, *For. Chronicle*, *69*(2), 187–192.
- Wotton, B., D. Martell, and K. Logan (2003), Climate change and people-caused forest fire occurrence in Ontario, *Clim. Change*, *60*, 275.
- Wu, S., L. Mickley, D. Jacob, J. Logan, R. Yantosca, and D. Rind (2007), Why are there large differences between models in global budgets of tropospheric ozone, *J. Geophys. Res.*, *112*, D05302, doi:10.1029/2006JD007801.
- Wu, S., L. J. Mickley, E. M. Leibensperger, D. J. Jacob, D. Rind, and D. G. Streets (2008), Effects of 2000–2050 global change on ozone air quality in the United States, *J. Geophys. Res.*, *113*, D06302, doi:10.1029/2007JD008917.
- Yevich, R., and J. Logan (2003), An assessment of biofuel use and burning of agricultural waste in the developing world, *Global Biogeochem. Cycles*, *17*(4), 1095, doi:10.1029/2002GB001952.

M. D. Flannigan, Great Lakes Forestry Centre, Canadian Forest Service, 1219 Queen Street East, Sault Ste. Marie, ON P6A 2E5, Canada.

R. C. Hudman, Department of Chemistry, University of California, Berkeley, CA 94720-1460, USA.

J. A. Logan, L. J. Mickley, and R. Yevich, School of Engineering and Applied Sciences, Harvard University, 109A Pierce Hall, 29 Oxford Street, Cambridge, MA 02138, USA.

D. V. Spracklen, Institute for Atmospheric Science, School of Earth and Environment, University of Leeds, Leeds LS2 9JT, UK. (d.spracklen@see.leeds.ac.uk)

A. Westerling, Sierra Nevada Research Institute, University of California, 5200 North Lake Road, Merced, CA 95343, USA.